AVANCES
EN CIENCIAS E INGENIERÍAS
ARTÍCULO/ARTICLE SECCIÓN/SECTION C

Atmospheric measurement station at Universidad San Francisco de Quito (EMA): ground-based physical meteorology instrumentation and assessment of initial measurements

Estación de mediciones atmosféricas en la Universidad San Francisco de Quito (EMA): instrumentación de meteorología física de la estación terrena y evaluación de mediciones iniciales

María Cazorla[1*], Esteban Tamayo[2]

[1] *Universidad San Francisco de Quito – Instituto de Investigaciones Atmosféricas - Colegio de Ciencias e Ingeniería Diego de Robles S/N, Cumbayá.*
[*] *Autor principal/Corresponding author, e-mail: cazorla.chem@gmail.com*

Editado por/Edited by: Cesar Zambrano, Ph.D.
Recibido/Received: 29/09/2014. Aceptado/Accepted: 07/10/2014.
Publicado en línea/Published on Web: 19/12/2014. Impreso/Printed: 19/12/2014.

Abstract

Meteorological variables in the valley of Cumbayá, Ecuador, are being monitored continuously at Universidad San Francisco de Quito's Atmospheric Measurement Station, EMA (Spanish acronym), since the end of May, 2014. Two months of data, June and July, were processed to assess instrument performance and data quality. A first look into the data sets shows that information generation is optimal. Data time series and monthly diurnal profiles for solar radiation flux density, ambient temperature, surface pressure, relative humidity, and wind speed and direction are presented. Wind rose plots show typical S, SE seasonality of summer winds. Finally, a 40.6 mm precipitation event on 23 May is shown.

Keywords. meteorology, Cumbayá, EMA, USFQ.

Resumen

Las variables meteorológicas en el valle de Cumbayá están siendo monitoreadas continuamente en la Estación de Mediciones Atmosféricas, EMA, de la Universidad San Francisco de Quito, desde fines de mayo de 2014. Dos meses de datos, junio y julio, fueron procesados a fin de evaluar el desempeño de los sensores y la calidad de los datos. Una primera mirada al juego de datos indica que la generación de información es óptima. En este trabajo se presentan series de tiempo y perfiles diurnos mensuales de flux de radiación solar, temperatura ambiente, presión, humedad relativa y velocidad y dirección del viento. Las rosas de viento muestran la estacionalidad S, SE de los vientos de verano. Finalmente se presenta un evento de precipitación de 40.6 mm de lluvia, que tuvo lugar el 23 de mayo.

Palabras Clave. meteorología, Cumbayá, EMA, USFQ.

Introduction

Continuous monitoring of meteorological variables is of major importance, as it is a source of first-hand information of current weather for the public and scientists who study atmospheric phenomena. In addition, weather observations from ground stations are critical inputs for numerical weather prediction models [1, 2]. In this regard, the number of regional ground stations that can supply models with high quality data has an impact on model results. Another factor is the temporal resolution of data collected at weather stations, since reliable sources of model boundary conditions imply availability and continuity of observational data. Furthermore, physical variables such as temperature, relative humidity, wind speed and direction, solar radiation and precipitation have an impact on the formation and dispersion of air pollutants in the ambient air [3]. Therefore, ground station measurements of meteorological variables provide the appropriate baseline information to interpret observations of air quality data [4] and to run chemical transport models [3, 5].

Environmental authorities in the city of Quito, through Secretaría del Ambiente, operate a monitoring network of air quality and physical meteorology variables within the city and its adjacent valleys [6]. The local network monitors weather and ambient air quality, and issues alerts for the population in the event of atmospheric conditions that could threaten public health. On the other

ISSN 1390-5384

hand, the Ecuadorian meteorological service (INAMHI) operates a nation-wide surface weather network, although online information is scarce and efforts to automate stations are recent. In spite of all these efforts, scientific research in the field of Atmospheric Science that involves specialized experimentation, data analysis and modeling is still a field to explore in Ecuador.

An atmospheric research facility, EMA (Spanish acronym for Atmospheric Measurement Station) began operations at Universidad San Francisco de Quito (USFQ) in February 2014. EMA was not conceived with the idea of becoming a meteorological or air quality service, although its baseline instrumentation can provide the public with useful information about the current weather. EMA has its origins in the need to acquire equipment and develop new techniques to conduct atmospheric research with the purpose of answering specific science questions.

The university's atmospheric measurement facility is located in one of Quito's densely populated outskirt valleys, Cumbayá. In this valley neither the local nor the national monitoring networks have placed automated weather or air quality stations. The observations taken with the EMA instruments, therefore, augment the local efforts to study the atmosphere.

Currently, specialized research is conducted at EMA. As a result, several pieces of meteorological and air quality instrumentation have been acquired. In addition, new techniques for atmospheric measurements are being developed. One of the baseline sets of measurements that are continuously taken is surface weather. In this article, an initial assessment of EMA's baseline meteorological data and instrument performance over a two-month period is presented.

Materials and Methods

EMA is sited on the roof of the Science and Engineering building at USFQ's main campus. The geographical coordinates of the roof-top facility are (0°11'47" S, 78°26'6" W), and altitude is 2391 masl. The roof is located at 11.5 m from the ground level. A map that shows EMA's location relative to the city of Quito is presented in Figure 1.

Figure 1: Location of USFQ's atmospheric measurement station (EMA) (blue balloon) relative to the city of Quito in Ecuador. EMA's geographical coordinates are (0°11'47" S, 78°26'6" W). Altitude is 2391 masl.

Measurements of meteorological variables are performed following technical criteria. Data quality is ensured through continuous monitoring of instrument performance [7].

Temperature and humidity are measured with a Vaisala HUMICAP probe, model HMP 155. The sensor has a radiation shield and is located at 2.40 m above the roof level, on the East side of the roof ledge. Instrument precision is +/- 1% for relative humidity, and +/- 0.2°C for typical ranges of temperature readings.

Direct and hemispherical solar radiation measurements are taken with a Kipp & Zonen pyranometer model CMP3, an ISO certified second class instrument with spectral range from 300 to 3000 nm, output sensitivity of 9.94 μV/(W m^{-2}), and accuracy better that 10%.

For precipitation, a Texas Electronic rain fall sensor model TR-525M with a reading accuracy of +/-1% is used. Surface pressure is measured with a Vaisala BAROCAP sensor with accuracy of +/- 0.3 hPa.

Wind speed and direction were first measured with a temporary Vaisala WM30 cup and vane wind sensor, until arrival of a Young 81000 ultrasonic anemometer on 15 June 2014. Wind measurements acquired with the first sensor were performed with an accuracy better that +/- 2% for speed, and +/- 3° for direction. The rate of acquisition was two data points per minute. In contrast, the Young anemometer takes readings with an accuracy of +/-1% for speed, +/- 2° for direction, and it is set to yield 1-second averages of 10 Hz data. All wind measurements have been taken with the sensor placed on a pole, 8.5 m above the roof level and 20 m above the ground level.

Data logging is being performed on a Vaisala MAWS301 automatic weather station. The sensors and data logger are sun-powered. The logger automatically processes data as 30-second averages and transmits information to the EMA's computer via a 232 communications port. All sensors were in-factory calibrated and delivered with their corresponding calibration certificates.

EMA began operations on 22 May 2014 and run in test mode for the rest of the month of May, until all sensors were online and yielding verified readings. Therefore, a set of 1-minute data averages for the months of June and July has been processed for solar radiation, temperature, pressure, relative humidity, wind speed, and wind direction. The data set consists of 42561 data points in June, and 43584 data points in July. Due to reasons related to EMA's technical operations, there was loss of data for less than half a day in June, and for over half a day in July. Regarding precipitation, the season has been mostly dry for which only one large event is reported on 23 May. In the following sections, time series

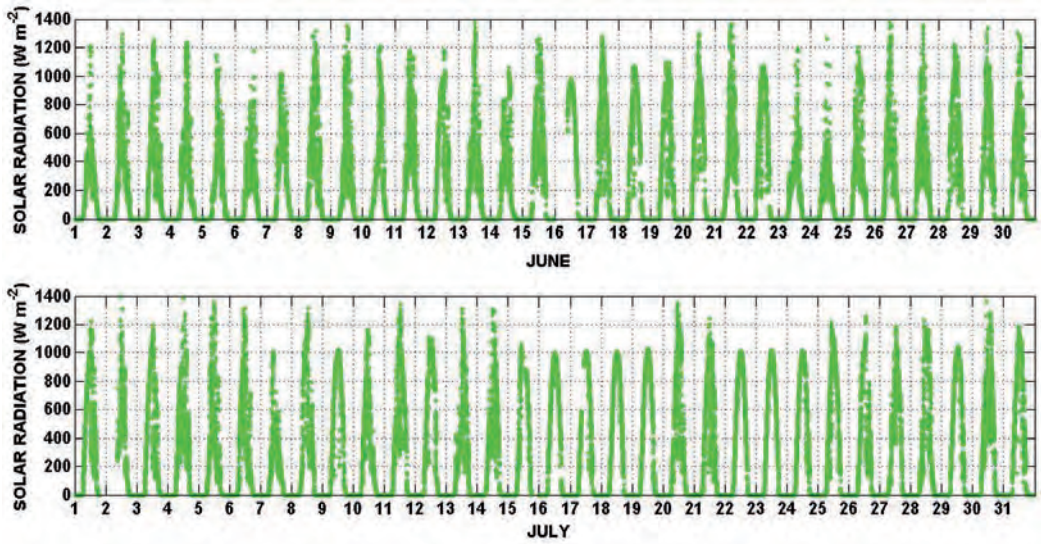

Figure 2: Time series of 1-minute solar radiation flux measured at EMA in Cumbayá, Ecuador, in June (upper panel) and July (bottom panel) 2014.

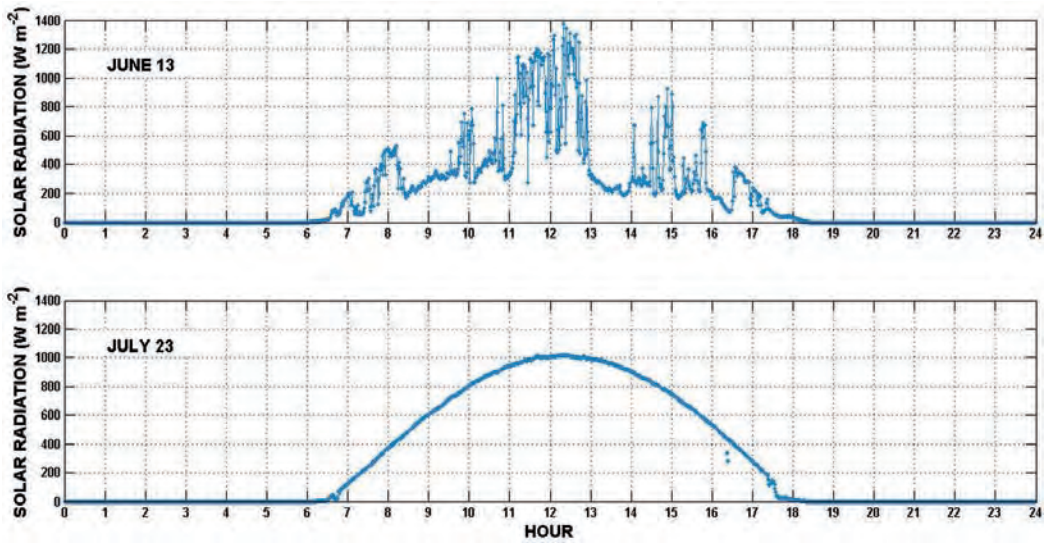

Figure 3: Examples of solar radiation flux diurnal profiles observed on 13 June (top panel) and 23 July (bottom panel). Both panels are zoomed-in graphs from time series in Figure 2.

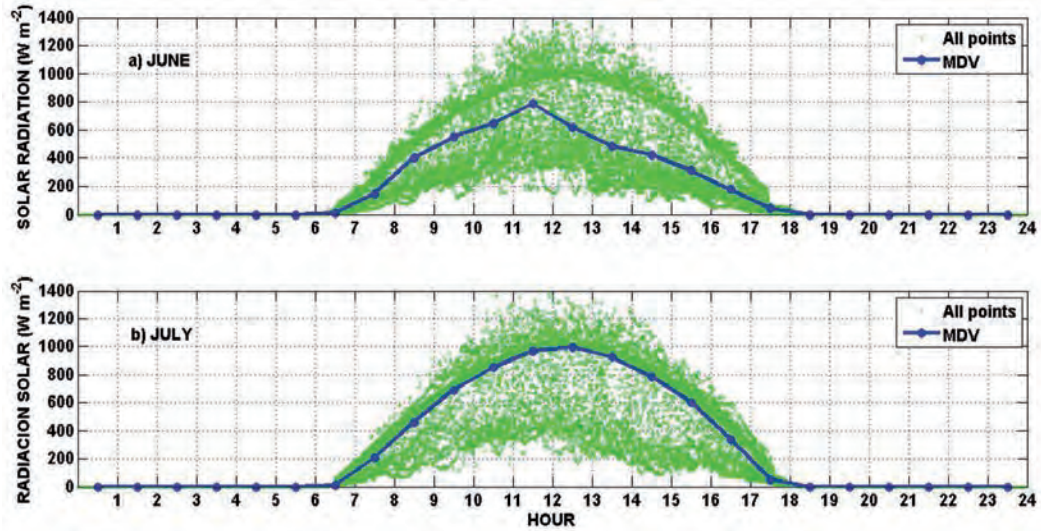

Figure 4: Diurnal profiles of solar radiation flux for a) June and b) July 2014, collected at EMA in Cumbayá, Ecuador. Green points are 1-minute data collected in a month and plotted against the hour of the day. The solid blue line is the monthly 1-hour median diurnal variation (MDV).

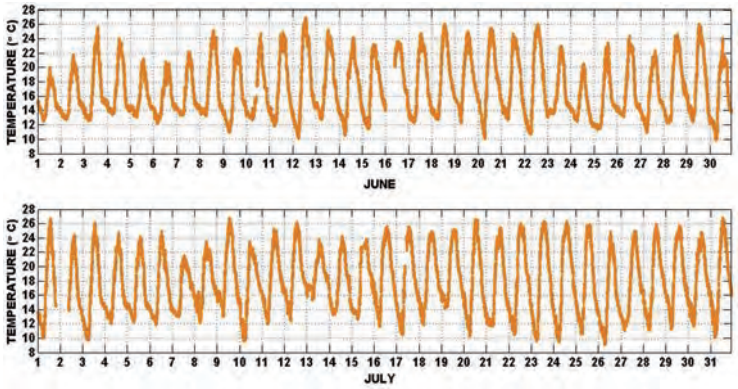

Figure 5: Time series of 1-minute temperature observations taken at EMA in Cumbayá, Ecuador, in June (upper panel) and July (bottom panel) 2014.

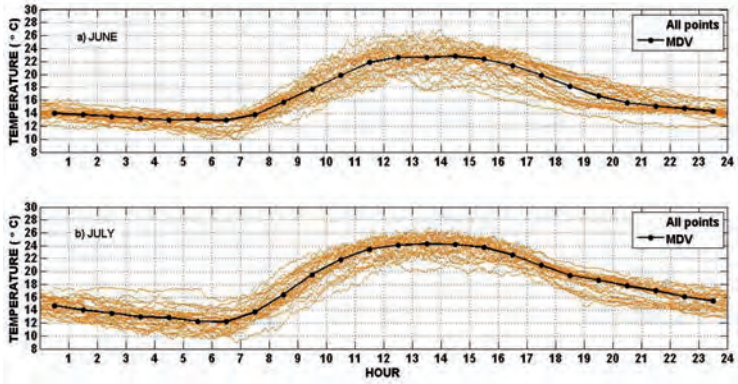

Figure 6: Temperature diurnal profiles for a) June and b) July 2014, collected at EMA in Cumbayá, Ecuador. Maroon points are 1-minute data points collected in one month and plotted against the hour of the day. The solid black line is the 1-hour median diurnal variation (MDV).

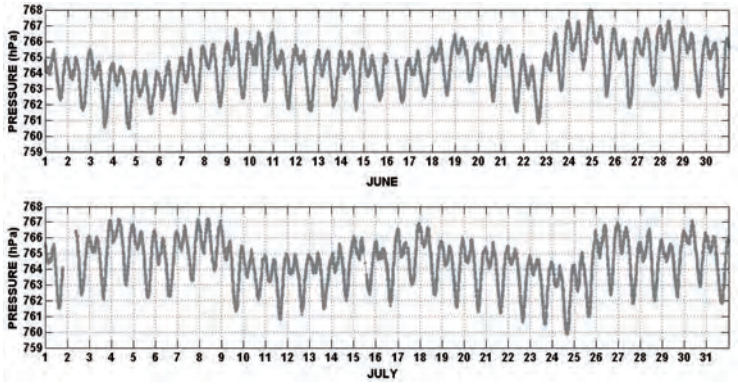

Figure 7: Time series of 1-minute atmospheric pressure observations taken at EMA in Cumbayá, Ecuador, in June (upper panel) and July (bottom panel) 2014.

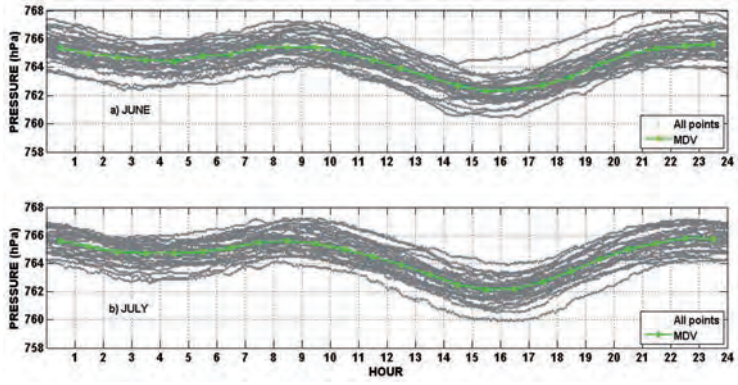

Figure 8: Atmospheric pressure diurnal profiles for a) June and b) July 2014, collected at EMA in Cumbayá, Ecuador. Grey points are 1-minute data points plotted against the hour of the day. The solid green line is the monthly 1-hour median diurnal variation (MDV).

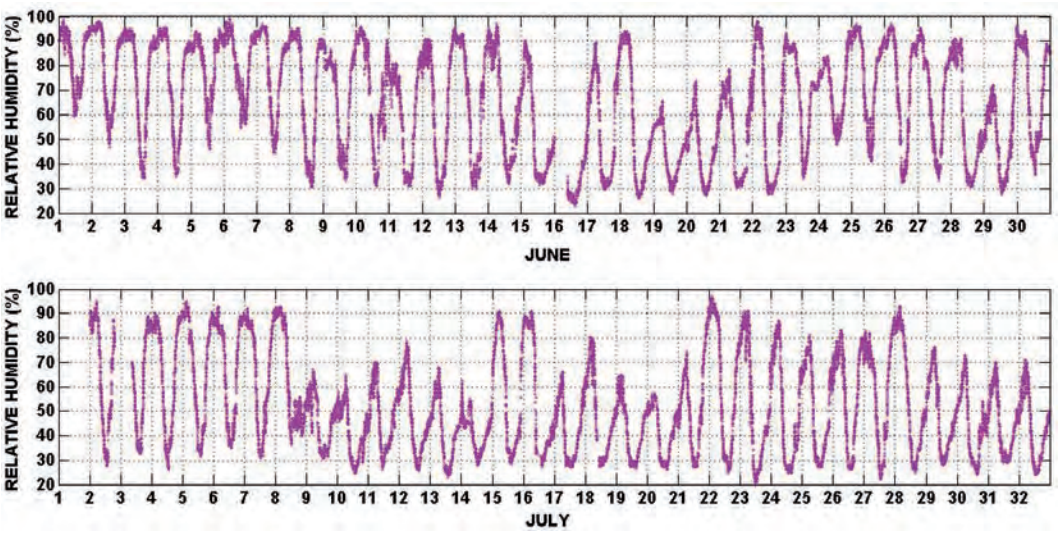

Figure 9: Time series of 1-minute relative humidity observations taken at EMA in Cumbayá, Ecuador, in June (upper panel) and July (bottom panel) 2014.

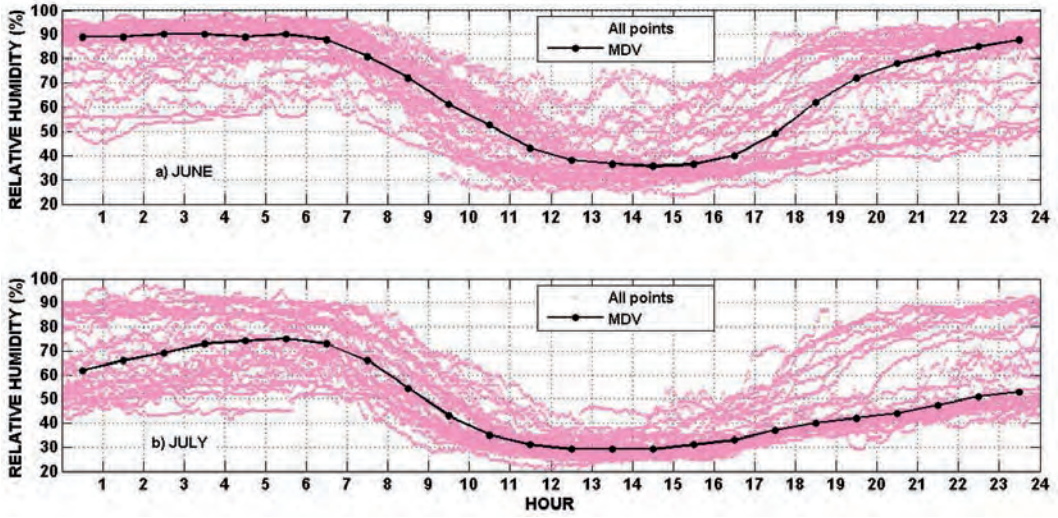

Figure 10: Relative humidity diurnal profiles for a) June and b) July 2014, collected at EMA in Cumbayá, Ecuador. Pink points are overlapped 1-minute averages plotted against the hour of the day. The solid black line is the hourly median diurnal variation (MDV).

and diurnal profiles of physical meteorology variables are presented.

Results and discussion

Solar radiation flux density

Solar radiation is the engine that initiates changes in weather and air pollution related phenomena. The availability of solar radiation flux density at the surface level at a given time, has a seasonal dependence on the solar declination angle, the latitude and the hour of the day [8]. In addition, atmospheric optical filters, cloud coverage, and particles in the atmosphere play a key role as absorption and scattering mechanisms attenuate the amount of light that reaches the surface at a given time. Detailed explanation on the transfer of solar radiation through the atmosphere can be found elsewhere [8, 9].

Time series of solar radiation flux density at the ground level in Cumbayá, during the months of June and July, are depicted in Figure 2. This measurements correspond to solar declinations going from 22.05° on 1 June at local hour 00h00, through 23.44° on 21 June (Northern Hemisphere summer solstice), to 18.01° on 31 July at local midnight. For the equatorial EMA's latitude (0°11'47" S) and at local noon, the solar zenith angle is practically equal to the solar declination angle [8].

Although in June and July there were as many as 10 days with solar radiation flux peaking between 1300 and 1400 Wm^{-2}, June was a cloudier month. Typical cloud structure in June and fair weather conditions in July are presented in Figure 3. For instance, in June there were intense solar radiation flux peaks, but there was also a substantial amount of cloudiness. An example can be observed on the top panel of Figure 3, for 13 June. On the other hand, clear days and days with fair weather clouds prevailed more consistently in July, in particular from the 15^{th} to the 26^{th}. An example of an almost perfect solar radiation profile is depicted for 23 July, on the bottom panel of Figure 3.

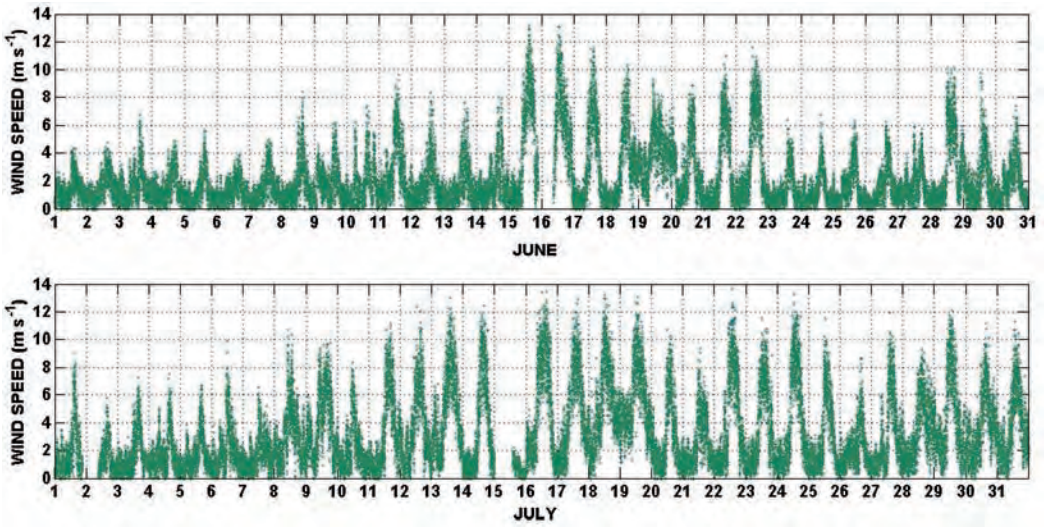

Figure 11: Time series of 1-minute wind speed observations at EMA in Cumbayá, Ecuador, during June (upper panel) and July (bottom panel) 2014.

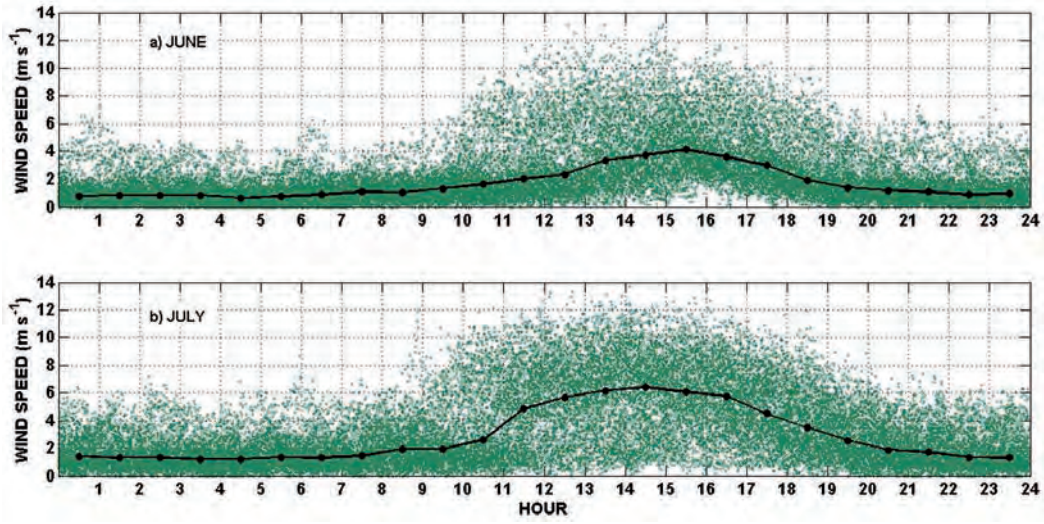

Figure 12: Wind speed diurnal ranges for a) June and b) July 2014, collected at EMA in Cumbayá, Ecuador. Dark green dots are 1-minute averages plotted against the hour of the day. The solid black line is the monthly 1-hour median diurnal variation (MDV).

Median diurnal variations (MDV) for solar radiation flux measurements were obtained overlapping data as function of the hour of the day and extracting the hourly median. Statistically, the median is an appropriate tool to obtain trends in meteorological data sets, since it effectively allows filtering data points that could otherwise bias the trend result. The MDV for June and July are represented with a solid blue line in Figure 4, a) for June, and b) for July. Looking at the MDVs on Figure 4, June cloudiness becomes evident, in particular in the afternoon hours, while the overall fair weather in July is similarly revealed.

Ambient air temperature

Temperature time series of 1-minute data collected at the EMA site during the months of June and July are depicted in Figure 5. In June, there were four days when temperature reached peaks greater or equal to 26°C. The warmest day was 12 June with a peak temperature of 27°C. On the other hand, temperature minima in this month ranged between 10 to 14°C, with only three days reaching the lowest value.

Further in the season, July turned into a warmer month with a total number of 11 days when the maximum temperature reached or surpassed 26°C. Regarding temperature minima, in July there were early morning temperatures lower than those recorded in June, and thus during seven days in July temperature minima were below 10°C.

Daytime ambient temperatures are correlated to the amount of solar radiation flux available at the surface level. As explained earlier, during the month of July there was less cloud coverage than in the month of June, which translated into higher daytime temperature readings. Similarly, less cloud coverage leads to faster radiative cooling of the surface during nighttime and early morning hours. Therefore, July's clearer skies became the underlying reason for lower temperature peaks during nights and early mornings.

Temperature MDVs for June and July are presented in

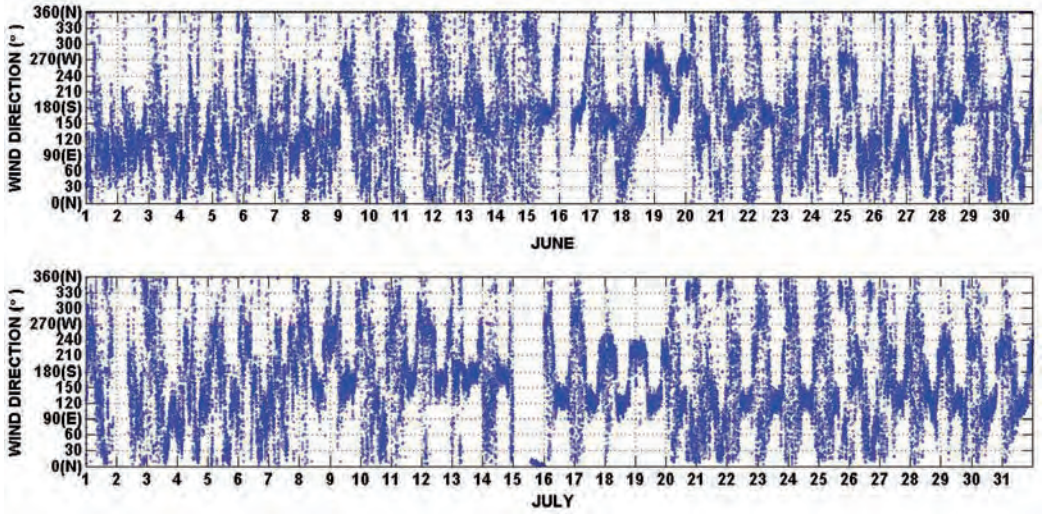

Figure 13: Time series of 1-minute wind direction observations at EMA in Cumbayá, Ecuador, during June (upper panel) and July (bottom panel) 2014.

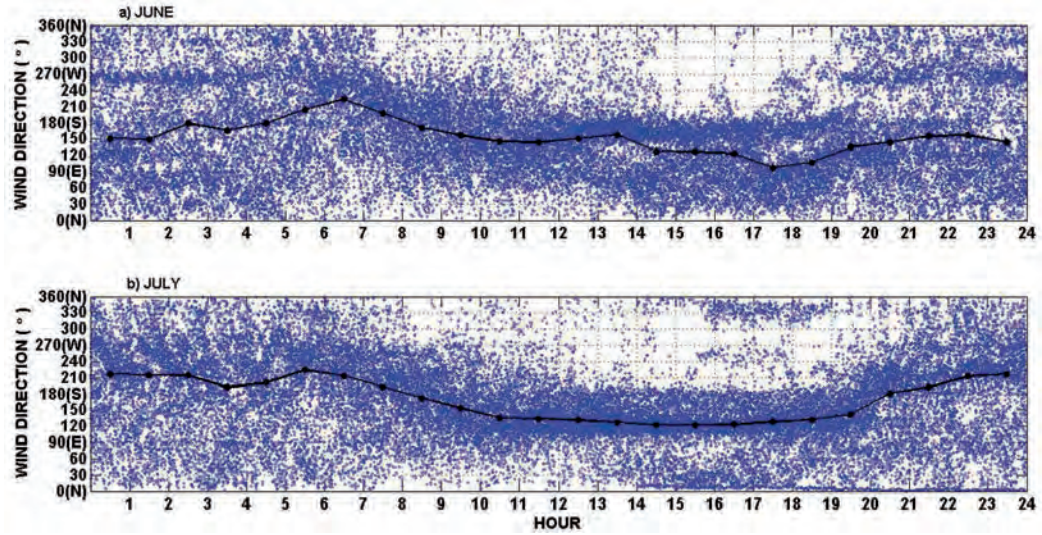

Figure 14: Wind direction diurnal trends for a) June and b) July 2014, collected at EMA in Cumbayá, Ecuador. Blue points are 1-minute data collected in a month and plotted against the hour of the day. The solid black line is the monthly 1-hour median diurnal variation (MDV).

Figure 6, a) and b). In June, packing of the points is less compact than in July, especially during the afternoon. Overall, in June temperature peaked at 22.6°C +/- 2.5°C at 14h00 local time, while in July the peak temperature was 24°C +/- 2°C, at the same hour.

Surface pressure

Atmospheric pressure variations at the surface level during June and July 2014 are presented in Figures 7 (time series) and 8 (MDVs). Overlapped time series data as a function of the hour of the day (Figure 8) reveal the cyclical atmospheric wave with a period of 12 hours, with troughs at local time 04h00 and 16h00, crests at 09h00 and around 22h00, and mean amplitude of about 1.6 hPa. This behavior reveals the known ground level print of the large scale movement of the atmosphere that yields a surface variation of pressure between 762 hPa to 765 hPa, Figure 8 a) and b), at the observation location.

Relative humidity

Relative humidity daily variations are correlated to temperature and solar radiation flux variations. In the nighttime and early morning, relative humidities are higher as temperature decreases in the absence of sunlight. Thermodynamically, lower temperatures shift the equilibrium vapor pressure to lower values, and so water vapor partial pressures divided by lower saturated vapor pressures yield higher relative humidities. Hence, relative humidity peaks occur between midnight and early morning hours, and lowest peaks occur at around 14h00, the time when temperature is maximum. Such diurnal variation can be observed in the time series presented in Figure 9, top and bottom panels for June and July, respectively. In July, the number of days with lower daytime and nighttime relative humidities is larger than in June, which relates to the fact that higher solar radiation fluxes at the surface level translate into warmer and drier air. This phenomena extends to some evenings through the night,

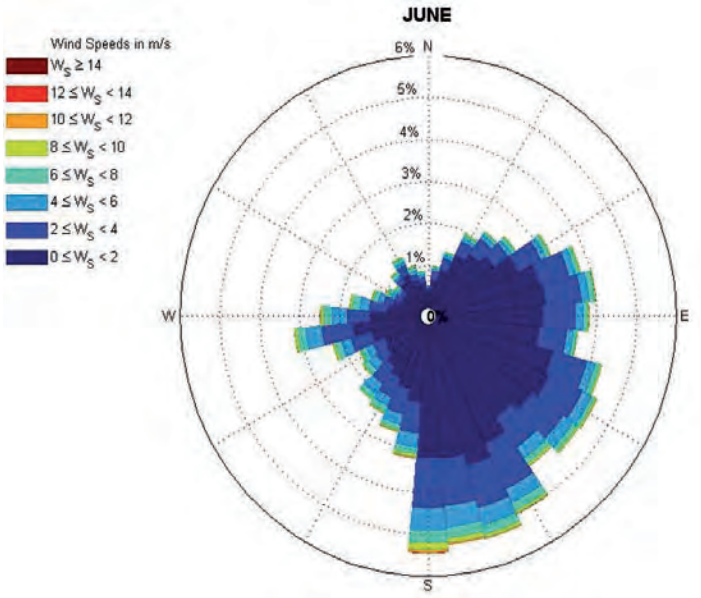

Figure 15: Wind rose plot obtained with 1-minute data for June 2014 collected at the EMA site in Cumbayá, Ecuador. Color palette indicates speed in m/s. Quadrants indicate wind direction. Radial scale indicates percentage of data points per bin.

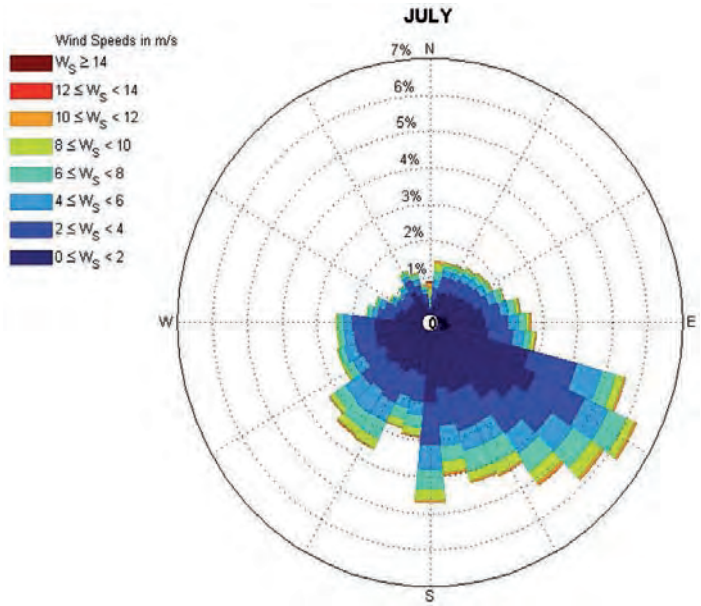

Figure 16: Wind rose plot obtained with 1-minute data for July 2014 collected at the EMA site in Cumbayá, Ecuador. Color palette indicates speed in m/s. Quadrants indicate wind direction. Radial scale indicates percentage of data points per bin.

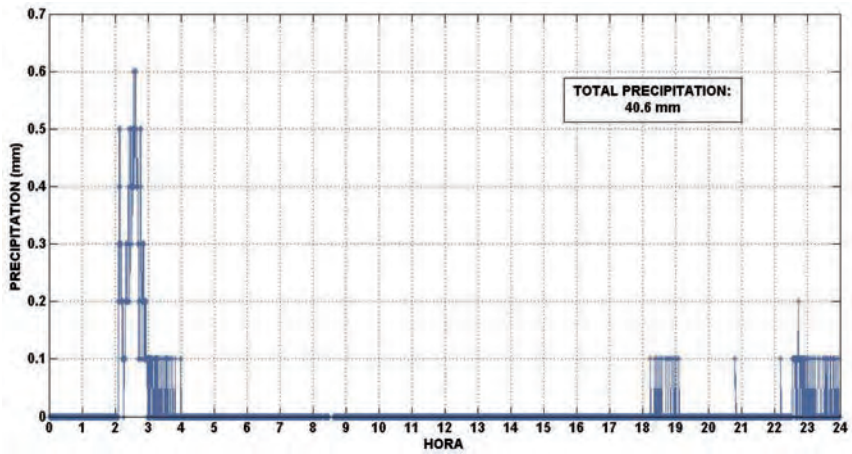

Figure 17: Large precipitation episode recorded at EMA on 23 May 2014 in Cumbayá, Ecuador. Total rainfall was 40.6 mm, out of which 33 mm correspond to the event between 02h06 and 03h35.

in particular between the 8^{th} to the 14^{th}, and between the 16^{th} to the 22^{nd} of July, when relative humidities in hours other than daylight hours were remarkably low. Overall, the hourly MDVs for relative humidity shown in Figure 10, indicate that a) in June the daytime minimum relative humidity was 37%, while b) in July it was 29% . On the other hand, during nighttime and early mornings, relative humidity most of the times was as high as 90% in June, Figure 10 a), while in July early morning relative humidity ranged between 60 and 72%, and reached 50% in the night, Figure 10 b).

Wind speed and direction

Surface observations of the wind field were also recorded for June and July 2014 at the EMA facility. June and July wind speed time series can be observed in Figure 11, top and bottom panels. Wind speeds reached afternoon peaks above 12 m s^{-1} in as many as 10 days in July, while June was less windy. Daily overlapping of the data shows the wind speed range during the months of June and July. This range is depicted collectively by the green dots in Figure 12, a) and b). Although overlapped points are more dispersed, if compared to the temperature data set, a diurnal profile is still apparent in Figures 12 a) and b). Median diurnal variations were obtained and depicted as solid black lines in Figure 12, even though trend values are statistically less significant than for temperature, due to larger data dispersion. Nevertheless, it is clear that 1) wind speed peaks at the time of peak temperature, and 2) in July wind speeds could be a factor of 1.5 higher than in June.

It is a known global circulation fact that during the Northern Hemisphere summer time, the Intertropical Convergence Zone (ITCZ) meanders a few degrees latitude to the North of the equator, mainly in the month of July [10]. As a result, at the surface level there is a strong meridional component of the wind vector that comes from the South. Combined with the easterlies around the equator, the main wind field during the Northern Hemisphere summer months come from the South East direction (SE), at the observation site. These phenomena is evident from the wind direction data collected at the EMA facility, in spite of the friction that wind is subject to at the ground level. Time series for wind direction during June and July are depicted on the top and bottom panels in Figure 13. Measurements of wind direction correspond to the value of the azimuthal angle, where the wind is blowing from, with the North marked at 0° and advancing clockwise, as the meteorological convention indicates. Monthly overlapped data presented in Figure 14, a) and b), show packing of data between 90° and 180°, mostly during daytime. As a result MDVs on the plots lay on the S, SE tick mark for daylight hours.

Wind speed and direction data were combined into wind rose plots for the months of June and July, as shown in Figures 15 and 16. A color scale was assigned to the magnitude of the wind vector, while direction is easily read from the corresponding plot quadrant. The radial scale corresponds to the percentage of data points for every blade-like bin. The June wind rose shows a larger overall percentage of data points for calm winds than in the month of July, when winds were more intense. Also the prevailing S, SE directions are clear from both wind roses, as it is seasonally expected.

Precipitation

Regarding rainfall measurements, June and July turned out to be dry summer months. The region received 11.6 mm of accumulated monthly precipitation in June, while in July rainfall was absent. However, on 23 May, the EMA precipitation sensor captured a major rainfall event that is worth mentioning. Figure 17 depicts the rain gauge readings for that event. On this day, a total of 40.6 mm of rain were recorded, out of which 33 mm correspond to a large thunderstorm that took place during the first hours of the day, between 02h06 and 03h35 local time.

Summary and future work

USFQ's EMA facility is acquiring real-time physical meteorology observations at the ground level in Cumbayá, Ecuador. Analysis of 1-minute data for June and July 2014 shows that at this temporal resolution measurement noise is low enough that further smoothing is unnecessary. From this perspective, baseline meteorology data is proven reliable and thus can be used as a basis for interpretation of additional atmospheric measurements.

From an operational standpoint, acquisition of the sonic anemometer data will be migrated from the Vaisala data logger to an independent and customized system. This step is necessary in order to avoid potential conflicts due to the anemometer's much faster sampling rates.

Seasonal changes of physical variables at the observation site are becoming evident from a first evaluation of the data sets. Continuous monitoring at fine temporal resolutions will allow building data records with substantial statistical significance. In this regard, further work involves coupling ground observations acquired at EMA with numerical weather prediction models. From the quality of the data, the outlook for successful modeling trials is promising.

Acknowledgements

Construction of the roof-top Atmospheric Measurement Station (EMA) at USFQ and acquisition of physical meteorology instrumentation were proposed by principal investigator M. Cazorla and funded by Universidad San Francisco de Quito. William H. Brune from the Department of Meteorology at Penn State University has supported research at EMA through donations and continuous science collaborations. We thank engineer Nelson Herrera for valuable and continuous advice. Engineer

Santiago Vargas provided technical support at the time of instrument setup. Volunteer students from the Department of Environmental Engineering have contributed to EMA's operations through the completion of various tasks.

References

[1] Daley, R. 1997. "Atmospheric Data Assimilation". *Journal of Meteorological Society of Japan*, 75(1B):209–219.

[2] Wallace, J.; Hobbs, P. 2006. "Atmospheric Science: an introductory survey". *Academic Press, Second Edition, Burlington*: 459–460.

[3] Seinfeld, J.; S., P. 2006. "Atmospheric chemistry from air pollution to climate change". *Wiley, Second Edition, USA*: 1092–1133.

[4] Heard, D. 2006. "Field Measurements of Atmospheric Composition". *en "Analytical techniques for atmospheric measurements", D. Heard (Ed.), Blackwell Publishing: Oxford*: 1–71.

[5] Bey, I.; Jacob, D.; Yantosca, R.; Logan, J.; Field, B.; Fiore, A.; Schultz, M. 2001. "Global modeling of tropospheric chemistry with assimilated meteorology: Model description and evaluation". *Journal of Geophysical Research: Atmospheres*, 106(D19):23073–23095.

[6] Distrito Metropolitano de Quito. 2013. "Informe Anual 2013. Calidad del Aire". *http://190.152.144.74/paginas/articulos.html*.

[7] Brock, F.; S., R. 2001. "Meteorological Measurement Systems". *Oxford University Press, Inc., New York*.

[8] Liou, K. 2002. "An Introduction to Atmospheric Radiation". *Academic Press, Second Edition, USA*: 44–50.

[9] Bohren, C.; Clothiaux, E. 2006. "Fundamentals of Atmospheric Radiation". *WILEY-VCH, Germany*.

[10] Waliser, D.; Gautier, C. 1993. "A satellite-derived climatology of the ITCZ". *Journal of Climate*, 6(11):2162–2174.